Applied Catalysis B: Environmental 245 (2019) 367–375

Contents lists available at ScienceDirect

Applied Catalysis B: Environmental

journal homepage: www.elsevier.com/locate/apcatb

# Production of hydrogen from brewery wastewater by aqueous phase reforming with Pt/C catalysts

A.S. Oliveira, J.A. Baeza, L. Calvo*, N. Alonso-Morales, F. Heras, J.J. Rodriguez, M.A. Gilarranz

*Departamento de Ingeniería Química, C/Francisco Tomás y Valiente 7, Universidad Autónoma de Madrid, 28049 Madrid, Spain*

ARTICLE INFO

*Keywords:*
Brewery wastewater
Aqueous phase reforming
Pt/C catalyst
Hydrogen

ABSTRACT

This paper reports for the first time on the aqueous phase reforming (APR) of a brewery wastewater, which was synthetically prepared according to a real effluent composition. Home-made Pt (3 wt. %) catalysts supported on different carbon materials, have been tested for this purpose at temperatures of 473 and 498 K. The effects of the supports and the organic load of the wastewater on the results of APR have been evaluated. Well characterized commercial carbons with different pH slurry and porous texture have been used as catalyst supports. A wide range of wastewater organic load has been tested, varying the COD from about 1500 to more than 11,200 mg/L, which corresponded to TOC values around 500 and more than 4000 mg/L, respectively. The highest removal of TOC and COD was observed for catalyst supported on highly mesoporous carbon blacks with virtually no microporosity and high pH slurry. At the lowest wastewater organic load (1531 mg/L $COD_{initial}$), TOC and COD removal up 99% was achieved and 93% of the TOC was converted into gases, with $H_2$ and alkanes representing more than 70% of the total gas volume generated. The removal of organic matter in the liquid phase decreased at increasing its concentration in the starting wastewater, although the resulting gas contained a higher percentage of $H_2$. Increasing the temperature allowed a higher TOC and COD removal, gas production, carbon conversion to gas and $H_2$ yield. Some deactivation of the catalysts was observed after five successive uses, which can be attributed to partial blockage of the active Pt sites by carbonaceous deposits. The results obtained allow considering APR as an environmentally promising solution for these biomass-derived wastewaters providing also an interesting way of valorisation to $H_2$-rich gas.

## 1. Introduction

Cortright et al. [1], in their pioneer work, showed that $H_2$ and alkanes can be produced with both high selectivity and yield from organic oxygenated compounds by aqueous phase reforming (APR) under mild reaction conditions (473–523 K, 15–50 bar) using supported metal catalysts. Since then, many studies have been carried out with different compounds or substrates such as alcohols, polyols, sugar [2–8], bio-oil [9,10], cellulose [11,12] and different types of lignocellulosic biomass [13,14], mainly for $H_2$ production. The results reported highlight the APR process as a promising way of producing fuels from renewable sources, although some studies have shown that the cost of the feedstock may be an important drawback for the application of APR [15]. The use of APR could be extended to biomass-derived wastewater treatment, thus integrating wastewater treatment and valorisation of residues. Industries producing large volumes of wastewater with high loads of biomass-derived organic compounds, such as the brewing plants, are interesting candidates for the implementation of the treatment of wastewater by APR. The brewing industry generates 3 to 10 L of wastewater per liter of beer produced [16]. Generally, breweries perform treatments consisting of physical, chemical and/or biological operations before discharge. In the literature, some works studied the application of biological treatments combined with energy production in the form of biogas rich in $CH_4$ or $H_2$ from brewery wastewater [17]. The studies on the possible application of APR as both wastewater treatment and valorisation method for the production of valuable gases are very scarce. Most of the literature on the APR is focused on model simple compounds and is addressed mainly to learn on the effect of the catalytic system and the reaction conditions on the performance of the process [18–20], while studies with more complex substrate are infrequent. There are only few studies that analyse the effect of impurities or mixtures of compounds on catalytic performance [21–25]. For instance, Lehnert and Claus [21], observed that the inorganic salts of crude glycerol strongly affect the catalytic activity, leading to lower $H_2$ production compared to pure glycerol. That loss of activity is probably due to catalyst poisoning by blockage of active sites. Boga et al. [22]

* Corresponding author.
*E-mail address:* luisa.calvo@uam.es (L. Calvo).

https://doi.org/10.1016/j.apcatb.2018.12.061
Received 4 October 2018; Received in revised form 17 December 2018; Accepted 23 December 2018
Available online 24 December 2018

also found similar results for APR of crude glycerol using 1 wt. % Pt on $Al_2O_3$ as catalyst. They reported that the $H_2$ selectivity decreased dramatically from 64 to 1% with pure glycerol and crude glycerol, respectively. The deactivation was caused by fatty acids, such as stearic and oleic and their salts, long chain alkanes and olefins, formed from the fatty acid derivatives in the feed, which can block partially the Pt active sites. The use of activated carbon, instead of $Al_2O_3$ as support significantly improved glycerol conversion and $H_2$ selectivity, due to adsorption of stearic acid on the carbon support. Remón et al. [23] analysed the effect of biodiesel-derived impurities ($CH_3OH$, $CH_3COOH$ and KOH) on the APR of glycerol. The presence of KOH increased gas production, whereas that of $CH_3COOH$ and $CH_3OH$ led to decreased gas production and glycerol conversion, respectively.

In addition to the composition of the substrate, the APR process is also strongly dependent on the catalytic system and the reaction conditions, including pressure, temperature and the type of reactor [4,18]. A diversity of catalytic systems, mainly based on VIII group metals, have been described in the literature for APR of oxygenated hydrocarbons [19,26,27]. Pt-based catalysts showed to be the most effective among monometallic catalysts in terms of activity and selectivity toward $H_2$-rich gas [19].

The catalytic support used may also have an impact on the APR process. Basic supports resulted in higher activity and $H_2$ yield, whereas acidic and neutral supports led to increased alkane formation [28]. Furthermore, the basic sites are of great significance for water–gas shift (WGS) reaction, playing a key role in the production of $H_2$, thus enhancing the performance of the APR process. Pt catalysts supported on solid basic oxides exhibited excellent activity in APR [29]and most of the publications on APR are focused on Pt supported on $\gamma$-$Al_2O_3$, due to the high selectivity to $H_2$ [2,20,30]. However, $\gamma$-$Al_2O_3$ has shown limited stability under APR conditions [20,30] and the activity of catalysts supported on $\gamma$-$Al_2O_3$ becomes generally poor when compared with those using other supports such as carbon materials [8]. Carbon materials have drawn attention as attractive supports in APR due to their high specific surface area, chemical and mechanical stability. Different types of activated carbons, carbon nanotubes and mesoporous carbons have been used as supports for APR catalysts [8,14,31–33]. The textural characteristics of the carbon support have also been found to have a strong influence on APR. Irregular pore arrangements, broad distribution of pore size and high microporosity have been reported to diminish the activity and reduce $H_2$ selectivity [32].

The aim of this work is to evaluate for the first time the treatment and valorisation of brewery wastewater through APR with Pt catalysts using different carbon materials as supports. The effects of support type and the organic load of the wastewater on the process performance have been investigated at two temperatures (473 and 498 K). Likewise, the stability of the catalyst showing the best performance was evaluated upon successive runs.

## 2. Experimental section

### 2.1. Materials

Hexachloroplatinic acid solution (8 wt. % in $H_2O$), malt extract, yeast extract, wheat peptone, maltose monohydrate, ammonium sulphate and ethanol were purchased from Sigma-Aldrich; di-sodium hydrogen phosphate and sodium di-hydrogen phosphate were purchased from Panreac. Commercial Norit®CAPSUPER activated carbon was supplied by Cabot Corporation (USA), ENSACO 250 G and 350 G carbon blacks were supplied by TIMCAL Canada Inc. (Canada) and mesoporous graphitized carbon black was supplied by Sigma-Aldrich (USA).

### 2.2. Preparation and characterization of supports and catalysts

Pt/C catalysts (3 wt. % Pt, carbon basis) were prepared by incipient wetness impregnation using commercial activated carbon (CAP), two carbon blacks (ENS250 and ENS350) and mesoporous graphitized carbon black (C-MESO) as supports. Impregnation was carried out using an aqueous solution of hexachloroplatinic acid. The impregnated samples were dried overnight in an oven at 333 K, calcined in air at 473 K during 2 h and then reduced under 25 N mL/min $H_2$ flow at 573 K during 2 h. The porous texture of the supports and catalysts was characterized by nitrogen adsorption-desorption at 77 K (Micromeritics TriStar II). The pH slurry of the carbon materials and catalysts was determined measuring, until constant value, the pH of an aqueous suspension of the materials in distilled water (1 g of solid per 10 mL of water). Scanning transmission electron microscopy (STEM) of the catalysts was performed using a JEOL - 3000 F at 300 kV microscope. Software 'ImageJ 1.51k' was used for counting and measuring Pt nanoparticles (NPs) on digital STEM images (more than 200 NPs were measured per catalyst).

CO adsorption measurements were recorded using the Micromeritics ASAP 2020C instrument. The metal dispersion on the support was evaluated from the amount of chemisorbed CO by assuming the stoichiometry of CO/Pt = 1. X-ray photoelectronic spectroscopy (XPS) profiles were recorded using a PHI VersaProbe II instrument equipped with X-ray excitation source, 1486.6 eV. Software 'XPS peak v4.1′ was used for the deconvolution of the spectra in order to obtain the relative amounts of $Pt^{n+}$ and $Pt^{\circ}$ species. The data analysis procedure involved smoothing, a Shirley background subtraction and mixed Gaussian–Lorentzian by a least-square method for curve fitting. C 1 s peak (284.6 eV) was used as internal standard for binding energies corrections due to sample charging.

### 2.3. Preparation and characterization of synthetic brewery wastewater

Synthetic brewery wastewater was prepared based on pH and typical concentrations of Biological Oxygen Demand (BOD), Chemical Oxygen Demand (COD) and nutrients found in real brewery wastewater [34]. The standard sample contained 1000 mg/L malt extract, 500 mg/L yeast extract, 150 mg/L peptone, 860 mg/L maltose, 1000 mg/L $(NH_4)_2SO_4$, 2.80 mL/L $C_2H_5OH$, 80 mg/L $NaH_2PO_4$ and 140 mg/L of $Na_2HPO_4$. The analytical characterization included Total Organic Carbon (TOC), using a TOC-VCSH apparatus (Shimadzu); COD, determined according to the standard method ASTM D1252, and ionic chromatography (IC) (883 Basic IC Plus, Metrohm) (Table S1, Supplementary Information). The TOC was close to 2000 mg/L and the COD was approximately 6200 mg/L, being the COD/TOC ratio about 3. This relatively high ratio suggests that there is a relative abundance of oxygen-containing organic species in the wastewater. The initial pH value was 6.9. The main anion species analysed by IC were chloride, glycolate, acetate, formate, phosphate and sulphate. Chloride was detected at low concentrations (4 mg/L), mainly ascribed to malt extract and peptone, which may contain chlorides. The glycolate concentration was 9 mg/L and acetate and formate were detected at much lower concentrations, not exceeding 1 mg/L, mainly ascribed to malt extract and maltose, which may contain different compounds including acetic, formic, fumaric, oxalic and glycolic acids. Phosphate and sulphate were the main anions (215 and 772 mg/L, respectively) since they were diretly introduced in the preparation of the synthetic wastewater.

In order to analyse the influence of organic load, wastewater samples with COD values within the usual range in breweries were prepared, diluting or concentrating the standard sample described above [34]. Table 1 shows the TOC and COD for all of the wastewater concentrations studied in this work.

### 2.4. Aqueous phase reforming experiments

APR runs were carried out batch wise in 50 mL stainless steel stoppered reactors (BR100, Berghoff). After previous experiments, the reaction time was established in 4 h, using 15 mL of brewery wastewater and 0.3 g of catalyst. The reactor was purged several times with

**Table 1**
TOC and COD of the synthetic wastewaters tested with different organic load.

| TOC (mg/L) | COD (mg/L) |
|---|---|
| 474 ± 47 | 1531 ± 120 |
| 974 ± 24 | 3046 ± 62 |
| 1968 ± 111 | 6229 ± 341 |
| 4124 ± 222 | 11,204 ± 1486 |

Ar before heating up and stirring (500 rpm). The experiments were performed at 473 and 498 K in order to study the effect of the reaction temperature. The total reaction pressure (24–29 bar) was the result of contribution of the vapour pressure of water, the pressure of the gases produced and the initial Ar pressure set at 10 bar for the experiments performed at 473 K and 5 bar for those conducted at 498 K.

After 4 h of reaction, the heating system was stopped and the reactor was cooled down to room temperature. The gases produced during the reaction were collected in multilayer foil sample bags (Supelco, USA). The volume was measured using a gas burette and it is expressed in normal conditions (NTP). The gases were analysed by a GC/FID/TCD (7820 A, Agilent) using 2 packed columns and a molecular sieve. This system allowed analysing $H_2$, CO, $CO_2$, $CH_4$ and $C_2H_6$. The final effluents of batch reactions were filtered and processed to measure TOC, COD and ionic species (IC). All APR experiments were performed at least by duplicate.

Catalyst stability was assessed in 5 cycles of use. After each cycle of use, the catalyst was separated by filtration and simply dried in an oven at 333 K overnight. Then it was used for the next cycle. Pt leaching was below the TXRF detection limits after the APR experiments, therefore leaching can be considered negligible.

The TOC and COD removal, carbon conversion to gas (*CC* gas) and $H_2$ yield ($Y_{H2}$) were calculated as:

$$\textbf{TOC or COD removal}\ (\%) = \frac{\mathbf{X_{initial\ (mg/L)}} - \mathbf{X_{final\ (mg/L)}}}{\mathbf{X_{initial\ (mg/L)}}} \times 100\% \quad (1)$$

where $X$ is the TOC or COD value,

$$\boldsymbol{CC\ gas}\ (\%) = \frac{\mathbf{C_{gas}\ (g)}}{\mathbf{C_{initial}\ (g)}} \times 100\% \quad (2)$$

$$Y_{H_2}\left(\mathrm{mmol}\Big/\mathrm{g}\,COD_i\right) = \frac{\mathrm{H_2\ (mmol)}}{\mathrm{COD_{initial}\ (g)}} \quad (3)$$

## 3. Results and discussion

### 3.1. Supports and catalysts characterization

Table 2 shows the BET surface area ($S_{BET}$), external or non-microporous area ($A_{ext}$), pore volume and pH slurry of the supports and catalysts. The CAP support yielded the highest surface area (1750 $m^2$ / g), followed by ENS350, also with a fairly high value (932 $m^2$/g). The ENS250 and C-MESO supports gave significantly lower surface area values (65 and 100 $m^2$/g, respectively). All the supports showed some contribution of mesoporosity and only CAP and ENS350 had a significant microporosity. The pH slurry varied from frankly acidic (CAP: 2.9) to slightly basic (C-MESO: 7.5) and basic (ENS250: 8.9, ENS350: 10.3). Impregnation with Pt did not produce any significant variation of the porous texture and pH slurry.

**Table 2**
Characterization of the carbon supports and catalysts.

| Samples | $S_{BET}$ ($m^2$/g) | $A_{ext}$ ($m^2$/g) | Micropore volume ($cm^3$/g) | Mesopore volume ($cm^3$/g) | pH slurry |
|---|---|---|---|---|---|
| CAP | 1750 | 706 | 0.48 | 0.75 | 2.6 |
| ENS250 | 65 | 65 | < 0.001 | 0.09 | 8.9 |
| ENS350 | 932 | 655 | 0.12 | 0.74 | 10.3 |
| C-MESO | 100 | 100 | < 0.001 | 0.25 | 7.5 |
| Pt/CAP | 1360 | 676 | 0.31 | 0.75 | 2.9 |
| Pt/ENS250 | 64 | 64 | < 0.001 | 0.09 | 8.6 |
| Pt/ENS350 | 901 | 623 | 0.12 | 0.69 | 9.9 |
| Pt/C-MESO | 90 | 90 | < 0.001 | 0,14 | 7.3 |

Fig. 1 shows STEM images and the corresponding size distribution of the Pt NPs of the catalysts. All of them showed quite similar values of mean NP size (within 4.0–4.7 nm), which were quite homogeneously distributed in all cases (standard deviation within 2.2–3.3 nm).

### 3.2. Performance of the Pt/C catalysts

#### 3.2.1. Effect of the support

The effect of the support on the performance of the catalysts in the APR of brewery wastewater ($COD_{initial}$ = 6229 mg/L) was investigated at 473 and 498 K. Fig. 2 shows the TOC and COD removal after the 4 h APR experiments. The results of blank tests (without catalysts) are also included. In general, the removal was higher at 498 K than at 473 K, which indicates that C—C and C—O bond cleavage is favoured by increasing the temperature [35] (Fig. 3).

Blank experiments resulted in TOC and COD removal values between 48–54 %, which can be partly ascribed to hydrothermal carbonization (HTC), since a dark brown solid was recovered by filtration after the treatment. Table S2 of Supplementary Information shows the elemental composition of the solid recovered after blank experiments, which is similar to those found in the literature for hydrochars [36]. The TOC and COD removal was improved from ca. 50% in blank runs to ca. 80% in catalyzed ones, particularly in the case of Pt/CAP, Pt/ENS250 and Pt/ENS350 catalysts. In spite of their significantly different surface area, these three catalysts showed quite similar efficiency for the conversion of the organic matter present in brewery wastewater upon APR. The porous texture neither seems to be a determining factor looking at the dramatically different pore size distribution of the microporous activated carbon (CAP) and the ENS250 carbon black and their similar results in terms of organic matter breakdown.

gure 3 depicts the concentrations of the main organic anions analysed in the initial and APR-treated wastewater (4 h). Other anionic species such as chloride, phosphate and sulphate were detected by IC, however, they were not significantly affected by the APR treatment. Only in the reactions carried out with Pt/CAP the phosphate concentration raised up to 1092–1263 mg / L, which can be ascribed to release from the support, which was manufactured by activation with phosphoric acid.

In the case of the blank experiments, the formate and glycolate concentrations decreased at higher temperature. Glycolic, acetic and formic acids are secondary/tertiary byproducts from glucose decay upon HTC. Glycolic acid can be produced through intermediates such as erythrose or glycolaldehyde, acetic acid through intermediates such as erythrose or 1,6-anhydro-glucose and formic acid through several intermediates such as erythrose, 1,6-anhydro-glucose, hydroxymethylfurfural or lactic acid [37]. This can explain the higher levels of glycolate, acetate and formate in these blank experiments, where HTC must be the main process. Glycolate, acetate and formate were detected in very low concentrations in the initial brewery wastewater and increased up to over 113–136 mg/L, 62–68 mg/L and 54–106 mg/L, respectively, in the blank experiments (equivalent to 7–9 % of TOC of the final liquid phase). Increasing the temperature, the glycolate concentration in the final effluent decreased (from 136 to 113 mg/L) as well as formate concentration (from 106 to 54 mg/L), while acetate concentration hardly varied. Higher temperatures generally increase gas production by HTC and it is more likely that glycolic and formic acids are converted to gaseous products [37,38]. Similar results were found by Quitain et al. [39] who reported that formic acid was readily produced at lower temperature but it easily decomposed at increasing

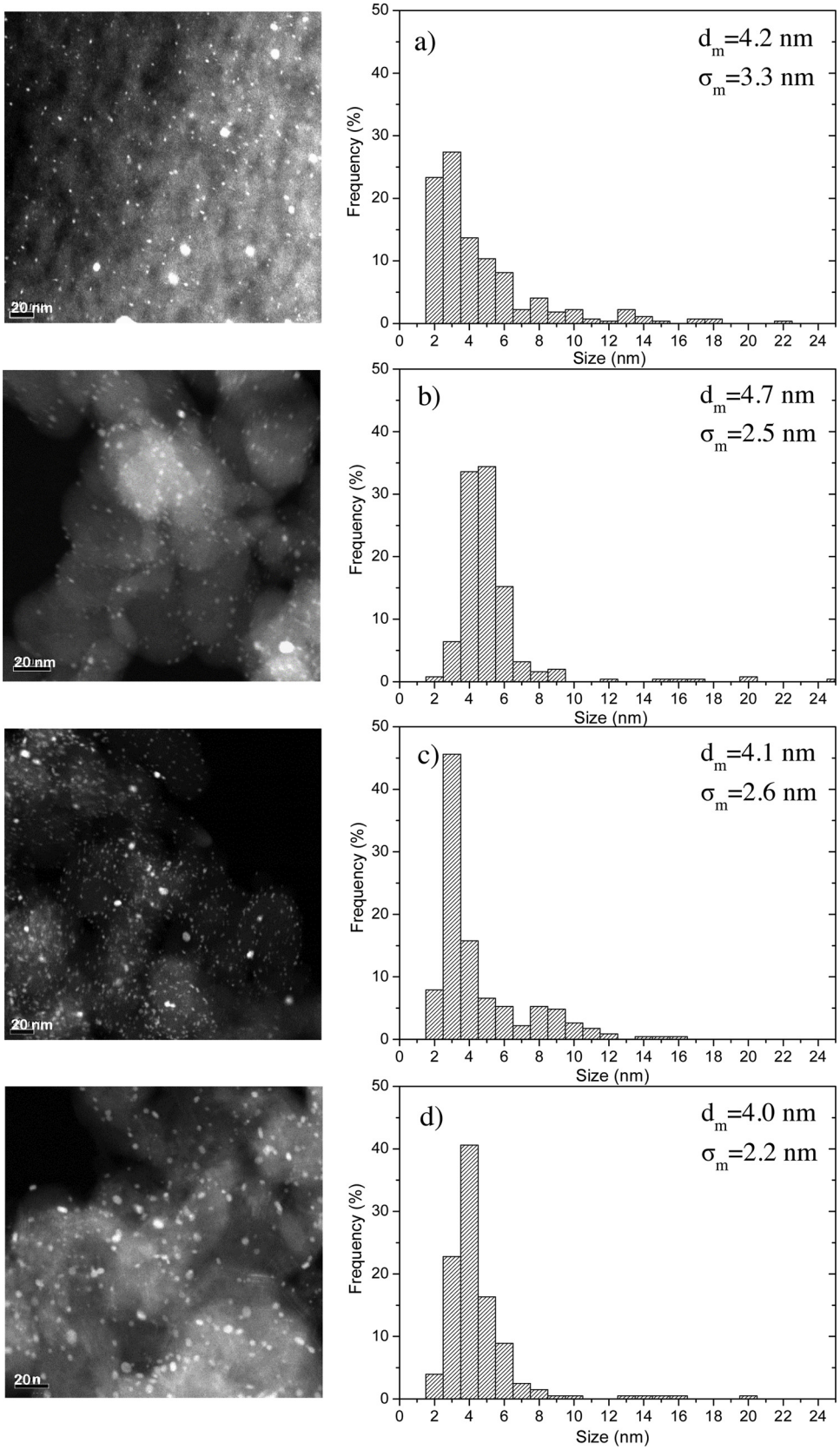


**Fig. 1.** STEM images of a) Pt/CAP, b) Pt/ENS250, c) Pt/ENS350 and d) Pt/C-MESO catalysts.

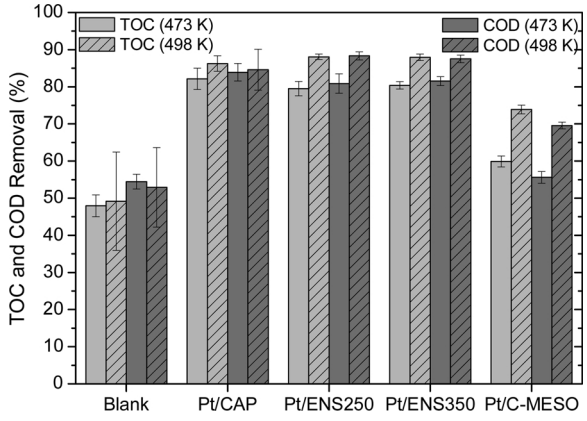


**Fig. 2.** TOC and COD removal after APR experiments at 473 and 498 K[a].
[a]Reaction conditions: initial Ar pressure: 10 bar at 473 K and 5 bar at 498 K; total reaction pressure: 24–29 bar; 15 mL of wastewater (1968 mg/L $TOC_{initial}$, 6229 mg/L $COD_{initial}$); 0,3 g catalyst; 500 rpm, 4 h.

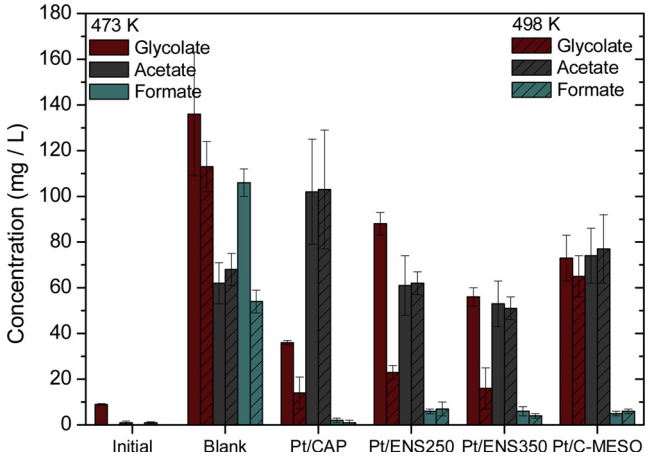


**Fig. 3.** Main anions detected by IC in the initial brewery wastewater and after APR experiments[a].
[a]Reaction conditions: initial Ar pressure: 10 bar at 473 K and 5 bar at 498 K; total reaction pressure: 24–29 bar; 15 mL of wastewater (1968 mg/L $TOC_{initial}$, 6229 mg/L $COD_{initial}$); 0,3 g catalyst; 500 rpm, 4 h.

temperature. Knezevic et al. [37] also found that acetic acid did not contribute to gas production, while glycolic and formic acids produced significant amounts of gas upon glucose conversion.

Catalytic APR can produce a diversity of oxygenated compounds (aldehydes, alcohols, carboxylic acids) as a result of series/parallel reactions such as dehydration or isomerization [40]. In the current work the amount of glycolate, acetate and formate detected corresponded to 7–15 % of TOC of the final effluent at 473 K and this proportion increased to 10–17 % at 498 K. Similar results were found by Remón et al. [41] who observed that at high catalyst/glycerol ratio increasing the temperature increased in the proportion of carboxylic acids in the liquid phase. Acetate was not converted easily upon the APR process with the Pt catalysts tested, indicating its refractory character under the operating conditions. The anions glycolate and formate were found at much lower concentrations than in the blank experiments since they can be reformed to $CO_2$ and $H_2$ and/or CO and $H_2O$. Additionally, it was observed that, except with the Pt/C-MESO catalyst, the final concentration of glycolate was significantly higher at lower temperature, an effect that was not observed for acetate and formate. Finally, the Pt/CAP catalyst produced a treated wastewater with a higher acetate and lower formate concentration than the other catalysts.

The main components identified in the gas fraction from APR were $H_2$, $CO_2$, $CH_4$ and $C_2H_6$ with all the catalysts tested. CO was only detected in the blank experiments, amounting between 5.3–5.5 % mol of the gas fraction. The virtual absence of CO in the catalysed experiments can be attributed to the activation of the WGS reaction by Pt. Table 3 shows the amount of gas produced and the composition of the gas fraction (except CO) obtained in the APR experiments together with the corresponding *CC gas* and $Y_{H2}$ values. Blank experiments produced a very low gas volume (2.2–3.3 mL), consisting mainly of $CO_2$, essentially ascribed to HTC [38]. Catalysed APR increased substantially the volume of gas produced (15.3–56.1 mL) with high percentage of valuable gases, $H_2$ and alkanes (41.7–71.6 %). It can be seen that the production of gases strongly depends on the catalyst used, thus indicating some important effects of the support. The reaction temperature is also important. At the highest temperature (498 K) the gas volume, the percentage of $H_2$ and therefore $Y_{H2}$, were significantly higher with all the catalysts, while the percentage of alkanes ($CH_4$ and $C_2H_6$) and $CO_2$ were smaller, due to a lower extent of methanation and alkanes formation reactions, which are thermodynamically favoured at lower temperatures. The value of *CC gas* also increased with temperature, consequently the remaining TOC of the liquid phase decreased, due to the favoured fragmentation of the organic matter through C—C and C–O bonds cleavage [35]. Although catalytic APR allowed always a significant increase of the *CC gas*, this varied within a fairly broad range (22.0–50.0 %) depending on the catalyst and temperature. Pt/ENS250 yielded the highest gas volume, *CC gas* and $H_2$ percentage in the gas fraction at the two temperatures tested. This catalyst was also the one for which the effect of temperature was more pronounced. Pt/C-MESO also allowed a high percentage of $H_2$ in the gas, although the gas volume obtained with this catalyst was lower. The percentage of $CH_4$ in the gas was higher with the Pt/CAP catalyst, representing more than 30% of that component in the gas fraction. The performance of Pt/ENS350 and Pt/C-MESO catalysts, in terms of gas production, *CC gas* and $Y_{H2}$, was quite similar.

The best performance observed for Pt/ENS250 could be partially attributed to the effect of the basic character of the support. This has been found to be beneficial for carbon conversion into gas products and $H_2$ formation [42], while acid supports have been reported to favour alkane formation [28]. Moreover, catalysts with basic sites improve the APR process through the promotion of the WGS reaction [29]. However, the basicity of the support must not be the only responsible of the better catalytic performance, since Pt/ENS350 has the support with the highest pH slurry but showed lower gas production, *CC gas* and $Y_{H2}$ than Pt/ENS250. The textural properties of the carbon support have also been claimed to strongly effect the results of APR [42]. Thus, some authors have associated the textural properties, such as irregular pore arrangement and high microporosity, to mass-transfer limitations [43,44]. Kim et al. [32] and Wang et al. [45] suggested that a high mesopore volume would facilitate the transport of reactants and products, whereas microporosity limits mass transfer, thus affecting to yield and products distribution. Likewise, Kim et al. [46] reported that in APR of glycerol mesoporous carbon-supported Pt catalysts showed better performance in terms of *CC gas*, $H_2$ selectivity, yield and $H_2$ production rate than Pt catalysts supported on commercial activated carbon of essentially microporous texture. Therefore, the best performance shown by Pt/ENS250 can be most likely associated to both the moderate basic character of the support and its mesoporous texture. The similar performance showed by Pt/C-MESO and Pt/ENS350 catalysts could be also explained by the mesoporous structure of the support C-MESO.

The maximum $Y_{H2}$ values in the APR of brewery wastewater were obtained with Pt/ENS250 at 498 K (293.9 mL $H_2$/g COD). Some works in literature studied the production of $H_2$ from brewery wastewater by batch anaerobic digestion [17]. At the optimum $H_2$ production conditions $Y_{H2}$ reached values of 149.6 mL $H_2$/g COD from a wastewater of similar composition to the one used in this work ($COD_{initial}$ = 6000 mg / L) [47]. Therefore, in this context the APR process clearly outperforms the production of $H_2$ by anaerobic digestion and shows an interesting

**Table 3**
Gas volume, composition of the gas fraction, *CC gas* and $Y_{H2}$ in the APR experiments[a].

| Catalyst | T (K) | Gas volume (mL) | Gas composition (% mol) | | | | *CC gas* (%) | $Y_{H2}$ (mmol $H_2$ / g $COD_i$) |
|---|---|---|---|---|---|---|---|---|
| | | | $H_2$ | $CO_2$ | $CH_4$ | $C_2H_6$ | | |
| Blank | 473 | 2.2 ± 0.4 | 2.2 ± 0.4 | 87.5 ± 3.7 | 3.3 ± 3.5 | 1.6 ± 1.9 | 3.8 ± 0.8 | < 0.1 |
| | 498 | 3.3 ± 0.7 | 4.2 ± 1.9 | 80.1 ± 5.6 | 8.2 ± 4.0 | 2.0 ± 0.2 | 5.7 ± 1.0 | 0.1 ± 0.1 |
| Pt/CAP | 473 | 17.7 ± 0.5 | 5.7 ± 2.7 | 58.3 ± 1.2 | 33.9 ± 1.7 | 2.2 ± 0.2 | 28.9 ± 0.1 | 0.4 ± 0.2 |
| | 498 | 23.1 ± 2.5 | 19.1 ± 1.0 | 48.6 ± 1.8 | 30.4 ± 0.9 | 2.0 ± 0.1 | 32.3 ± 3.0 | 2.0 ± 0.3 |
| Pt/ENS250 | 473 | 29.8 ± 2.1 | 35.4 ± 1.7 | 37.8 ± 3.6 | 23.9 ± 1.7 | 2.9 ± 0.2 | 34.0 ± 3.1 | 4.7 ± 0.1 |
| | 498 | 56.1 ± 4.6 | 48.9 ± 0.9 | 28.4 ± 0.5 | 21.0 ± 0.3 | 1.7 ± 0.1 | 50.0 ± 3.3 | 12.2 ± 1.2 |
| Pt/ENS350 | 473 | 15.3 ± 1.6 | 19.2 ± 0.9 | 54.0 ± 3.7 | 22.6 ± 2.3 | 4.2 ± 0.4 | 22.0 ± 2.4 | 1.3 ± 0.1 |
| | 498 | 28.6 ± 0.9 | 34.3 ± 0.7 | 41.7 ± 1.5 | 20.6 ± 0.6 | 3.3 ± 0.1 | 33.3 ± 1.3 | 4.4 ± 0.1 |
| Pt/C-MESO | 473 | 19.4 ± 1.4 | 33.2 ± 1.6 | 45.5 ± 3.2 | 18.5 ± 1.3 | 2.8 ± 0.2 | 22.9 ± 2.1 | 2.9 ± 0.1 |
| | 498 | 25.0 ± 1.0 | 41.1 ± 1.2 | 39.2 ± 2.0 | 17.1 ± 0.7 | 2.5 ± 0.1 | 26.0 ± 1.5 | 4.6 ± 0.1 |

[a] Reaction conditions: initial Ar pressure: 10 bar at 473 K and 5 bar at 498 K; total reaction pressure: 24–29 bar; 15 mL of wastewater (1968 mg/L $TOC_{initial}$, 6229 mg/L $COD_{initial}$); 0,3 g catalyst; 500 rpm, 4 h.

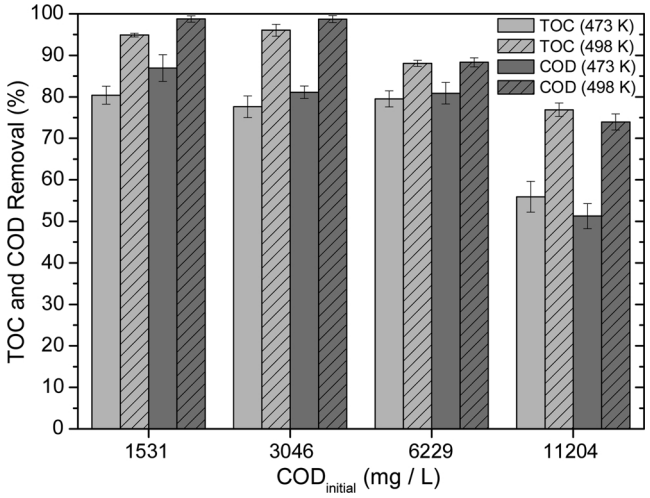


**Fig. 4.** TOC and COD removal upon APR at 473 and 498 K at different organic load[a].
[a]Reaction conditions: initial Ar pressure: 10 bar at 473 K and 5 bar at 498 K; total reaction pressure: 24–29 bar; 15 mL of wastewater; 0,3 g Pt/ENS250 catalyst; 500 rpm, 4 h.

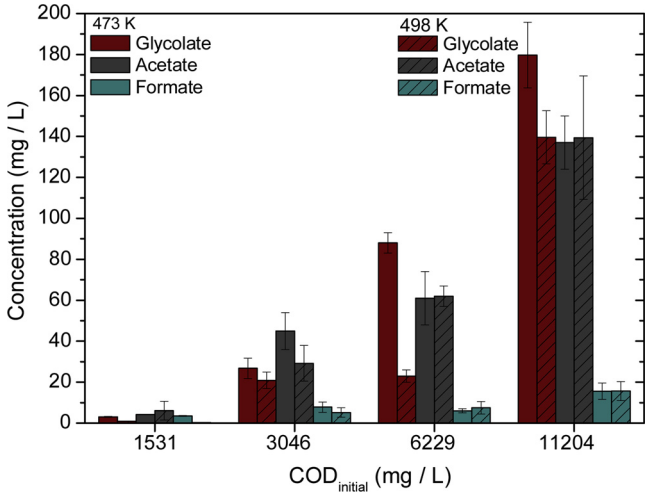


**Fig. 5.** Main anions detected at 473 and 498 K at different organic load[a].
[a]Reaction conditions: initial Ar pressure: 10 bar at 473 K and 5 bar at 498 K; total reaction pressure: 24–29 bar; 15 mL of wastewater; 0,3 g Pt/ENS250 catalyst; 500 rpm, 4 h.

potential for the treatment of wastewater. Moreover the gas heating values calculated from gas composition (Table 3) ranged within 2600–3200 kcal/kg, supporting the interest of the potential application of APR to this type of biomass derived wastewater.

### 3.2.2. Effect of the organic load

The effect of the organic load of the wastewater was investigated at the two temperatures of 473 and 498 K with the Pt/ENS250 catalyst, the one showing the best performance so far. Fig. 4 shows the values of TOC and COD removal at different starting organic loads. At the lowest organic load tested ($COD_{initial}$ = 1531 mg/L), removal values in the range of 80–99 % were obtained. Nearly identical removal rates were achieved when the $COD_{initial}$ was increased to 3046 mg/L, while at 11,204 mg/L of $COD_{initial}$, the TOC and COD removal decreased to 51–77 %. The trend observed is in good agreement with Kirilin et al. [35], who reported that the reforming of more concentrated feedstocks resulted in a reduction of the transformation of organic matter to gaseous products.

Fig. 5 depicts the concentration of the main organic anions detected after these APR experiments. Increasing the starting concentration from 1531 to 11,204 mg/L $COD_{initial}$ caused a clear increase of the final concentration of anionic species in the liquid phase. The concentration of glycolate, acetate and formate reached maximum values of 180, 139 and 16 mg/L, respectively. No significant differences were observed in the individual anions species with temperature, except for glycolate in some cases. However, the relative amount of these species with respect to TOC increased with the temperature at all organic loads tested, varying within 4–51 % of TOC in the final effluent. Moreover, increasing the starting COD from 3046 to 11,204 mg/L caused a decrease of the final proportion of these species, respect to TOC, from 51% to 12% at 498 K. In this sense, Remón et al. [41] also observed that the proportion of carboxylic acids in the liquid phase decreased at increasing concentration of glycerol.

Table 4 shows the gas volume produced, the *CC gas*, the composition of the gas fraction and the $Y_{H2}$ obtained in the experiments of Fig. 4. The gas volume produced increased gradually at increasing organic loads, up to a value of 59.7 mL at the highest concentration and temperature tested. No systematic trends could be observed respect to the composition of the gaseous products at 473 K. However, in the experiments carried out at 498 K, the percentage of $H_2$ increased monotonically with the starting organic load of the wastewater, reaching almost 50% at the highest $COD_{initial}$ tested. An opposite trend was observed for alkanes ($CH_4$ and $C_2H_6$) although of relatively low significance. In a previous work on the APR of glycerol, Luo et al. [20] reported that increasing the feed concentration of glycerol from 5 to 10 wt. % increased by about 10% the $H_2$ selectivity while slightly decreasing the selectivity to $CH_4$. The *CC gas* and $Y_{H2}$ decreased gradually at increasing the starting organic load, which is in good agreement with the reported by Luo et al. [20]. For the lowest wastewater

**Table 4**
Gas volume, composition of the gas fraction, *CC gas* and $Y_{H2}$ at different organic load[a].

| $COD_{initial}$ (mg/L) | T (K) | Gas volume (mL) | Gas composition (% mol) | | | | *CC gas* (%) | $Y_{H2}$ (mmol $H_2$/g $COD_i$) |
|---|---|---|---|---|---|---|---|---|
| | | | $H_2$ | $CO_2$ | $CH_4$ | $C_2H_6$ | | |
| 1531 ± 120 | 473 | 17.1 ± 1.1 | 40.7 ± 1.9 | 35.4 ± 3.5 | 22.0 ± 1.4 | 1.9 ± 0.1 | 73.4 ± 6.9 | 12.6 ± 0.2 |
| | 498 | 21.0 ± 0.8 | 40.5 ± 1.1 | 35.0 ± 2.0 | 20.8 ± 0.8 | 3.6 ± 0.1 | 93.0 ± 4.9 | 15.4 ± 0.2 |
| 3046 ± 62 | 473 | 24.0 ± 1.6 | 44.2 ± 2.2 | 32.0 ± 3.8 | 22.1 ± 1.5 | 1.8 ± 0.1 | 47.3 ± 4.8 | 9.7 ± 0.2 |
| | 498 | 33.0 ± 1.1 | 46.7 ± 1.2 | 30.0 ± 2.0 | 21.2 ± 0.7 | 2.1 ± 0.1 | 62.3 ± 3.3 | 14.0 ± 0.1 |
| 6229 ± 341 | 473 | 29.8 ± 2.1 | 35.4 ± 1.7 | 37.8 ± 3.6 | 23.9 ± 1.7 | 2.9 ± 0.2 | 34.0 ± 3.1 | 4.7 ± 0.1 |
| | 498 | 56.1 ± 4.6 | 48.9 ± 0.9 | 28.4 ± 0.5 | 21.0 ± 0.3 | 1.7 ± 0.1 | 50.0 ± 3.3 | 12.2 ± 1.2 |
| 11,204 ± 1486 | 473 | 33.2 ± 1.8 | 34.1 ± 1.2 | 43.5 ± 2.4 | 19.7 ± 1.0 | 2.7 ± 0.1 | 18.4 ± 1.3 | 2.8 ± 0.1 |
| | 498 | 59.7 ± 1.3 | 49.4 ± 0.8 | 30.6 ± 1.3 | 17.8 ± 0.4 | 2.2 ± 0.1 | 25.4 ± 0.9 | 7.3 ± 0.1 |

[a] Reaction conditions: initial Ar pressure: 10 bar at 473 K and 5 bar at 498 K; total reaction pressure: 24–29 bar; 15 mL of wastewater; 0,3 g Pt/ENS250 catalyst; 500 rpm, 4 h.

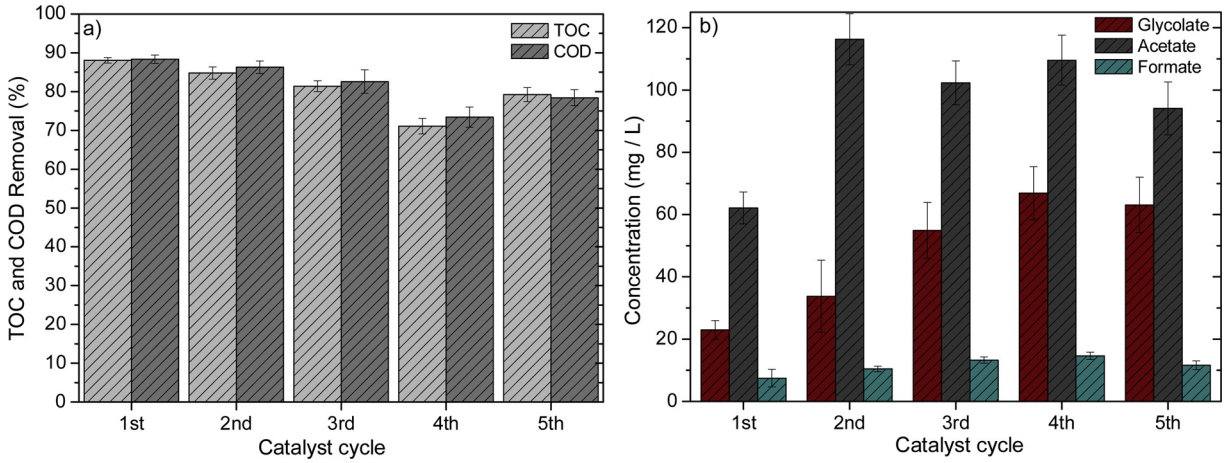


**Fig. 6.** a) TOC and COD removal and b) anions detected upon 5 successive APR cycles[a].
[a]Reaction conditions: temperature: 498 K; initial Ar pressure: 5 bar; total reaction pressure: 26–29 bar; 15 mL of wastewater (1968 mg/L $TOC_{initial}$, 6229 mg/L $COD_{initial}$); 0,3 g Pt/ENS250 catalyst; 500 rpm, 4 h.

concentration, *CC gas* values up to 73.4% and 93.0% were obtained at 473 and 498 K, respectively, while those values decreased dramatically (18.4% and 25.4%) at the highest organic load tested. Similar trend was observed for $Y_{H2}$, with also a pronounced decrease when increasing the COD of the starting wastewater.

### 3.2.3. Catalyst stability

The stability of the Pt/ENS250 catalyst was investigated upon 5 successive APR cycles (4 h reaction each) at 498 K with the starting wastewater at 6229 mg/L of COD. Fig. 6a) shows the results obtained based on TOC and COD removal and b) referred to the main organic anions detected. The removal of TOC and COD decreased slowly along the 4 first cycles and then recovered although to values somewhat below those of the fresh catalyst. These results indicate a fairly stable performance of the catalyst, supported also by the evolution of the anionic species given in Fig. 6b).

The gas volume produced, the composition of the gas fraction, the $Y_{H2}$ and the *CC gas* obtained in each cycle are summarized in Table 5. The production of gases and the *CC gas* decreased monotonically upon the cycles, showing these results a poorer stability of the catalyst than the suggested by the previous ones based on TOC and COD removal. As a result of the lower production of gases, $Y_{H2}$ also decreased gradually up to about one half of the obtained with the fresh catalysts after the 5th cycle. However, the results on the composition of the gas fraction were more stable, with a relatively small decrease of $H_2$ (≈ 10%) and a moderate increase of $CO_2$ (≈ 25%) in the gas composition.

To learn more on the performance of the catalyst upon successive cycles, the fresh and used Pt/ENS250 were characterized by adsorption-desorption of nitrogen, STEM, XPS and CO chemisorption. The results are collected in Table 6. The BET surface area remained almost constant

**Table 5**
Gas volume, composition of the gas fraction, *CC gas* and $Y_{H2}$ obtained upon 5 successive APR cycles[a].

| Catalyst cycle | Gas volume (mL) | Gas composition (% mol) | | | | *CC gas* (%) | $Y_{H2}$ (mmol $H_2$ /g $COD_i$) |
|---|---|---|---|---|---|---|---|
| | | $H_2$ | $CO_2$ | $CH_4$ | $C_2H_6$ | | |
| 1st | 56.1 ± 4.6 | 48.9 ± 0.9 | 28.4 ± 0.5 | 21.0 ± 0.3 | 1.7 ± 0.1 | 50.0 ± 3.3 | 12.2 ± 1.2 |
| 2nd | 48.6 ± 0.8 | 47.7 ± 0.6 | 30.9 ± 0.9 | 19.5 ± 0.3 | 1.9 ± 0.1 | 44.6 ± 1.2 | 10.3 ± 0.1 |
| 3rd | 40.2 ± 1.0 | 46.9 ± 0.9 | 31.8 ± 1.5 | 19.3 ± 0.5 | 2.0 ± 0.1 | 37.4 ± 1.6 | 8.4 ± 0.1 |
| 4th | 37.5 ± 0.7 | 46.3 ± 0.7 | 31.6 ± 1.1 | 20.0 ± 0.4 | 2.1 ± 0.1 | 35.3 ± 1.1 | 7.7 ± 0.1 |
| 5th | 29.2 ± 1.1 | 43.6 ± 1.3 | 35.7 ± 2.1 | 18.5 ± 0.7 | 2.2 ± 0.1 | 34.7 ± 1.7 | 6.8 ± 0.1 |

[a] Reaction conditions: temperature: 498 K; initial Ar pressure: 5 bar; total reaction pressure: 26–29 bar; 15 mL of wastewater (1968 mg/L $TOC_{initial}$, 6229 mg/L $COD_{initial}$); 0,3 g Pt/ENS250 catalyst; 500 rpm, 4 h.

**Table 6**
Characterization of the fresh and used Pt/ENS250 catalyst upon 5 successive APR cycles[a].

| Catalysts | Mean Pt NPs Size[b] (nm) | $S_{BET}$ ($m^2$/g) | $Pt^{n+}$ / $Pt^{\circ}$ ratio | Pt dispersion[c] (%) |
|---|---|---|---|---|
| initial | 4.7 ± 2.5 | 64 | 0.2 | 21 |
| after 1st cycle | 5.2 ± 2.8 | 63 | 0.6 | – |
| after 3rd cycle | 5.5 ± 3.3 | 61 | 0.5 | 9 |
| after 5th cycle | 6.5 ± 3.9 | 61 | 0.6 | 3 |

[a] Reaction conditions: temperature: 498 K; initial Ar pressure: 5 bar; total reaction pressure: 26–29 bar; 15 mL of wastewater (1968 mg/L $TOC_{initial}$, 6229 mg/L $COD_{initial}$); 0,3 g Pt/ENS250 catalyst; 500 rpm, 4 h.
[b] From STEM images.
[c] From CO chemisorption.

upon use. The electrodeficient to zerovalent Pt ratio increased after the 1st cycle but then remained almost constant, so that it cannot be conclusively associated to the loss of catalytic activity. The mean size of Pt NPs, as obtained from STEM, suffered only a slow monotonical increase. However, major changes were evidenced by CO chemisorption. Pt dispersion decreased dramatically, which is not consistent with the particle size obtained by STEM. These discrepancies can be explained through the formation of carbonaceous deposits covering Pt NPs, thus hindering CO chemisorption. That would explain the decreased activity with a lower effect on the selectivity [48]. Interestingly, deactivation of the catalyst by acetic acid has been also observed in reforming reactions with Pt-based catalysts, promoting the generation of coke precursors [49].

## 4. Conclusion

The APR of brewery wastewater was studied for the first time using Pt catalysts (3 wt. %) supported on different carbon materials. Two working temperatures 473 and 498 K were tested. In the absence of catalysts, HTC was the main process, leading to moderate TOC and COD removal (48–54 %) and fairly low production of gas consisting mainly of $CO_2$. With the Pt/C catalysts tested, APR led to substantially higher TOC and COD removal, with some significant differences between the catalysts depending on the carbon support used. The highest values of gas production were obtained with Pt/ENS250 at 498 K, possibly due to the effect of the basic character and the mesoporous texture of the support (a non-microporous commercial carbon black).

The organic load (expressed as COD) of the starting wastewater exerts a significant influence on the catalytic performance and the results of APR. At the lowest wastewater concentration (1531 mg /L of $COD_{initial}$), TOC and COD removal values up 99% were obtained, while at the highest concentration (11,204 mg/L of $COD_{initial}$), these values were reduced dramatically to 51%. However, the percentage of $H_2$ in the gas fraction increased with the concentration of the wastewater. The results indicate that APR can be a promising technology for biomass-derived wastewater through the production of $H_2$ and alkanes.

The activity of the catalysts decreased upon successive cycles of use, although no substantial changes were observed in the composition of the gas produced. Formation of carbonaceous deposits on the metal surface, appears a main cause of catalyst deactivation. The loss of activity affected mostly to the gas production and the $H_2$ yield and in a much lower extent to the removal of TOC and COD from the wastewater.

## Acknowledgements

The authors greatly appreciate financial support from Spanish MINECO (CTQ2015-65491-R). A. S. Oliveira thanks the Spanish MINECO a research grant (BES-2016-077244).

## Appendix A. Supplementary data

Supplementary material related to this article can be found, in the online version, at doi:https://doi.org/10.1016/j.apcatb.2018.12.061.

## References

[1] R.D. Cortright, R.R. Davda, J.A. Dumesic, Hydrogen from catalytic reforming of biomass-derived hydrocarbons in liquid water, Nature 418 (2002) 964–967, https://doi.org/10.1038/nature01009.
[2] J.W. Shabaker, R.R. Davda, G.W. Huber, R.D. Cortright, J.A. Dumesic, Aqueous-phase reforming of methanol and ethylene glycol over alumina-supported platinum catalysts, J. Catal. 215 (2003) 344–352, https://doi.org/10.1016/S0021-9517(03)00032-0.
[3] R.R. Davda, J.A. Dumesic, Renewable hydrogen by aqueous-phase reforming of glucose, Chem. Commun. 10 (2004) 36–37, https://doi.org/10.1002/anie.200353050.
[4] A. Iriondo, J.F. Cambra, V.L. Barrio, M.B. Guemez, P.L. Arias, M.C. Sanchez-Sanchez, R.M. Navarro, J.L.G. Fierro, Glycerol liquid phase conversion over monometallic and bimetallic catalysts: effect of metal, support type and reaction temperatures, Appl. Catal. B Environ. 106 (2011) 83–93, https://doi.org/10.1016/j.apcatb.2011.05.009.
[5] A.V. Kirilin, A.V. Tokarev, L.M. Kustov, T. Salmi, J.-P. Mikkola, D.Y. Murzin, Aqueous phase reforming of xylitol and sorbitol: comparison and influence of substrate structure, Appl. Catal. A Gen. 435–436 (2012) 172–180, https://doi.org/10.1016/j.apcata.2012.05.050.
[6] T. Nozawa, Y. Mizukoshi, A. Yoshida, S. Naito, Aqueous phase reforming of ethanol and acetic acid over TiO2 supported Ru catalysts, Appl. Catal. B Environ. 146 (2014) 221–226, https://doi.org/10.1016/j.apcatb.2013.06.017.
[7] Y. Wei, H. Lei, Y. Liu, L. Wang, L. Zhu, X. Zhang, G. Yadavalli, B. Ahring, S. Chen, Renewable hydrogen produced from different renewable feedstock by aqueous-phase reforming process, J. Sustain. Bioenergy Syst. 4 (2014) 113–127, https://doi.org/10.4236/jsbs.2014.42011.
[8] M.C. Kim, T.W. Kim, H.J. Kim, C.U. Kim, J.W. Bae, Aqueous phase reforming of polyols for hydrogen production using supported Pt-Fe bimetallic catalysts, Renew. Energy 95 (2016) 396–403, https://doi.org/10.1016/j.renene.2016.04.020.
[9] C. Pan, A. Chen, Z. Liu, P. Chen, H. Lou, X. Zheng, Aqueous-phase reforming of the low-boiling fraction of rice husk pyrolyzed bio-oil in the presence of platinum catalyst for hydrogen production, Bioresour. Technol. 125 (2012) 335–339, https://doi.org/10.1016/j.biortech.2012.09.014.
[10] A. Chen, P. Chen, D. Cao, H. Lou, Aqueous-phase reforming of the low-boiling fraction of bio-oil for hydrogen production: the size effect of Pt/Al2O3, Int. J. Hydrogen Energy 40 (2015) 14798–14805, https://doi.org/10.1016/j.ijhydene.2015.09.030.
[11] G. Wen, Y. Xu, Z. Xu, Z. Tian, Direct conversion of cellulose into hydrogen by aqueous-phase reforming process, Catal. Commun. 11 (2010) 522–526, https://doi.org/10.1016/j.catcom.2009.12.008.
[12] T. Soták, M. Hronec, I. Vávra, E. Dobročka, Sputtering processed tungsten catalysts for aqueous phase reforming of cellulose, Int. J. Hydrogen Energy 41 (2016) 21936–21944, https://doi.org/10.1016/j.ijhydene.2016.08.183.
[13] B. Meryemoglu, B. Kaya, S. Irmak, A. Hesenov, O. Erbatur, Comparison of batch aqueous-phase reforming of glycerol and lignocellulosic biomass hydrolysate, Fuel. 97 (2012) 241–244, https://doi.org/10.1016/j.fuel.2012.02.011.
[14] B. Kaya, S. Irmak, A. Hasanoğlu, O. Erbatur, Developing Pt based bimetallic and trimetallic carbon supported catalysts for aqueous-phase reforming of biomass-derived compounds, Int. J. Hydrogen Energy 40 (2015) 3849–3858, https://doi.org/10.1016/j.ijhydene.2015.01.131.
[15] D.A. Sladkovskiy, L.I. Godina, K.V. Semikina, E.V. Sladkovskaya, D.A. Smirnova, D.Y. Murzin, Process design and techno-economical analysis of hydrogen production by aqueous phase reforming of sorbitol, Chem. Eng. Res. Des. 134 (2018) 104–116, https://doi.org/10.1016/j.cherd.2018.03.041.
[16] G.S. Simate, J. Cluett, S.E. Iyuke, E.T. Musapatika, S. Ndlovu, L.F. Walubita, A.E. Alvarez, The treatment of brewery wastewater for reuse: state of the art, Desalination 273 (2011) 235–247, https://doi.org/10.1016/j.desal.2011.02.035.
[17] M.K. Arantes, H.J. Alves, R. Sequinel, E.A. da Silva, Treatment of brewery wastewater and its use for biological production of methane and hydrogen, Int. J. Hydrogen Energy 42 (2017) 26243–26256, https://doi.org/10.1016/j.ijhydene.2017.08.206.
[18] I. Coronado, M. Stekrova, M. Reinikainen, P. Simell, L. Lefferts, J. Lehtonen, A review of catalytic aqueous-phase reforming of oxygenated hydrocarbons derived from biorefinery water fractions, Int. J. Hydrogen Energy 41 (2016) 11003–11032, https://doi.org/10.1016/j.ijhydene.2016.05.032.
[19] R.R. Davda, J.W. Shabaker, G.W. Huber, R.D. Cortright, J.A. Dumesic, A review of catalytic issues and process conditions for renewable hydrogen and alkanes by aqueous-phase reforming of oxygenated hydrocarbons over supported metal catalysts, Appl. Catal. B Environ. 56 (2005) 171–186, https://doi.org/10.1016/j.apcatb.2004.04.027.
[20] N. Luo, X. Fu, F. Cao, T. Xiao, P.P. Edwards, Glycerol aqueous phase reforming for hydrogen generation over Pt catalyst – effect of catalyst composition and reaction conditions, Fuel 87 (2008) 3483–3489, https://doi.org/10.1016/j.fuel.2008.06.021.
[21] K. Lehnert, P. Claus, Influence of Pt particle size and support type on the aqueous-phase reforming of glycerol, Catal. Commun. 9 (2008) 2543–2546, https://doi.org/10.1016/j.catcom.2008.07.002.

[22] D.A. Boga, F. Liu, P.C.A. Bruijnincx, B.M. Weckhuysen, Aqueous-phase reforming of crude glycerol: effect of impurities on hydrogen production, Catal. Sci. Technol. 6 (2016) 134–143, https://doi.org/10.1039/C4CY01711K.
[23] J. Remón, J. Ruiz, M. Oliva, L. García, J. Arauzo, Effect of biodiesel-derived impurities (acetic acid, methanol and potassium hydroxide) on the aqueous phase reforming of glycerol, Chem. Eng. J. 299 (2016) 431–448, https://doi.org/10.1016/j.cej.2016.05.018.
[24] J. Remón, C. Jarauta-Córdoba, L. García, J. Arauzo, Effect of acid (CH3COOH, H2SO4and H3PO4) and basic (KOH and NaOH) impurities on glycerol valorisation by aqueous phase reforming, Appl. Catal. B Environ. 219 (2017) 362–371, https://doi.org/10.1016/j.apcatb.2017.07.068.
[25] A. Seretis, P. Tsiakaras, Crude bio-glycerol aqueous phase reforming and hydrogenolysis over commercial SiO2-Al2O3 nickel catalyst, Renew. Energy 97 (2016) 373–379, https://doi.org/10.1016/j.renene.2016.05.085.
[26] J.N. Chheda, G.W. Huber, J.A. Dumesic, Liquid-phase catalytic processing of biomass-derived oxygenated hydrocarbons to fuels and chemicals, Angew. Chemie - Int. Ed. 46 (2007) 7164–7183, https://doi.org/10.1002/anie.200604274.
[27] R.R. Davda, J.W. Shabaker, G.W. Huber, R.D. Cortright, J.A. Dumesic, Aqueous-phase reforming of ethylene glycol on silica-supported metal catalysts, Appl. Catal. B Environ. 43 (2003) 13–26, https://doi.org/10.1016/S0926-3373(02)00277-1.
[28] G. Wen, Y. Xu, H. Ma, Z. Xu, Z. Tian, Production of hydrogen by aqueous-phase reforming of glycerol, Int. J. Hydrogen Energy 33 (2008) 6657–6666, https://doi.org/10.1016/j.ijhydene.2008.07.072.
[29] Y. Guo, M.U. Azmat, X. Liu, Y. Wang, G. Lu, Effect of support's basic properties on hydrogen production in aqueous-phase reforming of glycerol and correlation between WGS and APR, Appl. Energy 92 (2012) 218–223, https://doi.org/10.1016/j.apenergy.2011.10.020.
[30] K. Koichumanova, A.K.K. Vikla, D.J.M. de Vlieger, K. Seshan, B.L. Mojet, L. Lefferts, Towards stable catalysts for aqueous phase conversion of ethylene glycol for renewable hydrogen, ChemSusChem 6 (2013) 1717–1723, https://doi.org/10.1002/cssc.201300445.
[31] K.E. Jeong, H.D. Kim, T.W. Kim, J.W. Kim, H.J. Chae, S.Y. Jeong, C.U. Kim, Hydrogen production by aqueous phase reforming of polyols over nano- and micro-sized mesoporous carbon supported platinum catalysts, Catal. Today 232 (2014) 151–157, https://doi.org/10.1016/j.cattod.2014.02.005.
[32] T.-W. Kim, H.-D. Kim, K.-E. Jeong, H.-J. Chae, S.-Y. Jeong, C.-H. Lee, C.-U. Kim, Catalytic production of hydrogen through aqueous-phase reforming over platinum/ordered mesoporous carbon catalysts, Green Chem. 13 (2011) 1718, https://doi.org/10.1039/c1gc15235a.
[33] D.J.M. de Vlieger, L. Lefferts, K. Seshan, Ru decorated carbon nanotubes – a promising catalyst for reforming bio-based acetic acid in the aqueous phase, Green Chem. 16 (2014) 864–874, https://doi.org/10.1039/c3gc41922c.
[34] H. Habte Lemji, H. Eckstädt, A pilot scale trickling filter with pebble gravel as media and its performance to remove chemical oxygen demand from synthetic brewery wastewater, J. Zhejiang Univ. B (Biomed. Biotechnol.) 14 (2013) 924–933, https://doi.org/10.1631/jzus.B1300057.
[35] A.V. Kirilin, A.V. Tokarev, E.V. Murzina, L.M. Kustov, J.P. Mikkola, D.Y. Murzin, Reaction products and transformations of intermediates in the aqueous-phase reforming of sorbitol, ChemSusChem 3 (2010) 708–718, https://doi.org/10.1002/cssc.200900254.
[36] H. Simsir, N. Eltugral, S. Karagoz, Hydrothermal carbonization for the preparation of hydrochars from glucose, cellulose, chitin, chitosan and wood chips via low-temperature and their characterization, Bioresour. Technol. 246 (2017) 82–87, https://doi.org/10.1016/j.biortech.2017.07.018.
[37] D. Knežević, W.P.M. van Swaaij, S.R.A. Kersten, Hydrothermal conversion of biomass: I, glucose conversion in hot compressed water, Ind. Eng. Chem. Res. 48 (2009) 4731–4743, https://doi.org/10.1021/ie801387v.
[38] A. Funke, F. Ziegler, Hydrothermal carbonization of biomass: a summary and discussion of chemical mechanisms for process engineering, Biofuels, Bioprod. Biorefining 4 (2010) 160–177, https://doi.org/10.1002/bbb.198.
[39] A.T. Quitain, M. Faisal, K. Kang, H. Daimon, K. Fujie, Low-molecular-weight carboxylic acids produced from hydrothermal treatment of organic wastes, J. Hazard. Mater. 93 (2002) 209–220, https://doi.org/10.1016/S0304-3894(02)00024-9.
[40] J.W. Shabaker, J.A. Dumesic, Kinetics of aqueous-phase reforming of oxygenated hydrocarbons: Pt/Al2O3 and Sn-Modified Ni catalysts, Ind. Eng. Chem. Res. 43 (2004) 3105–3112, https://doi.org/10.1021/ie049852o.
[41] J. Remón, J.R. Giménez, A. Valiente, L. García, J. Arauzo, Production of gaseous and liquid chemicals by aqueous phase reforming of crude glycerol: influence of operating conditions on the process, Energy Convers. Manage. 110 (2016) 90–112, https://doi.org/10.1016/j.enconman.2015.11.070.
[42] L.I. Godina, A.V. Kirilin, A.V. Tokarev, I.L. Simakova, D.Y. Murzin, Sibunit-supported mono- and bimetallic catalysts used in aqueous-phase reforming of xylitol, Ind. Eng. Chem. Res. 57 (2018) 2050–2067, https://doi.org/10.1021/acs.iecr.7b04937.
[43] S.H. Joo, K. Kwon, D.J. You, C. Pak, H. Chang, J.M. Kim, Preparation of high loading Pt nanoparticles on ordered mesoporous carbon with a controlled Pt size and its effects on oxygen reduction and methanol oxidation reactions, Electrochim. Acta 54 (2009) 5746–5753, https://doi.org/10.1016/j.electacta.2009.05.022.
[44] Y.G. Wang, L. Cheng, F. Li, H.M. Xiong, Y.Y. Xia, High electrocatalytic performance of Mn3O4/mesoporous carbon composite for oxygen reduction in alkaline solutions, Chem. Mater. 19 (2007) 2095–2101, https://doi.org/10.1021/cm062685t.
[45] X. Wang, N. Li, Z. Zhang, C. Wang, L.D. Pfefferle, G.L. Haller, High-yield hydrogen production from aqueous phase reforming over single-walled carbon nanotube supported catalysts, ACS Catal. 2 (2012) 1480–1486, https://doi.org/10.1021/cs300274m.
[46] T.W. Kim, H.J. Park, Y.C. Yang, S.Y. Jeong, C.U. Kim, Hydrogen production via the aqueous phase reforming of polyols over three dimensionally mesoporous carbon supported catalysts, Int. J. Hydrogen Energy 39 (2014) 11509–11516, https://doi.org/10.1016/j.ijhydene.2014.05.106.
[47] X.Y. Shi, D.W. Jin, Q.Y. Sun, W.W. Li, Optimization of conditions for hydrogen production from brewery wastewater by anaerobic sludge using desirability function approach, Renew. Energy 35 (2010) 1493–1498, https://doi.org/10.1016/j.renene.2010.01.003.
[48] L.I. Godina, A.V. Tokarev, I.L. Simakova, P. Mäki-Arvela, E. Kortesmäki, J. Gläsel, L. Kronberg, B. Etzold, D.Y. Murzin, Aqueous-phase reforming of alcohols with three carbon atoms on carbon-supported Pt, Catal. Today 301 (2018) 78–89, https://doi.org/10.1016/j.cattod.2017.03.042.
[49] D.J.M. De Vlieger, B.L. Mojet, L. Lefferts, K. Seshan, Aqueous phase reforming of ethylene glycol - role of intermediates in catalyst performance, J. Catal. 292 (2012) 239–245, https://doi.org/10.1016/j.jcat.2012.05.019.